

Electrodeposition of Zn-Co-Mo Alloy on the Steel Substrate from Citrate Bath and Its Corrosion Behavior in the Chloride Media

A. Keyvani, M. Yeganeh, and H. Rezaeyan

(Submitted October 30, 2016; in revised form March 4, 2017; published online March 20, 2017)

In this study, Zn-Co-Mo coatings were deposited on the steel substrate from a citrate bath after adjusting pH, concentration, and current density. The morphology, the content of alloying elements, and the thickness of deposits were studied. Deposition behavior of these ternary coatings was examined by cathodic polarization and cyclic voltammetry (CV) techniques. The synthesized deposits were investigated by scanning electron microscopy (SEM), energy-dispersive x-ray (EDX) analysis, x-ray diffraction (XRD), electrochemical impedance spectroscopy (EIS), and potentiodynamic polarization methods. The results showed that the deposition potential of Zn-Co-Mo alloy was feasible in negative potentials higher than about -1.25 V versus Ag/AgCl. Moreover, the corrosion behavior of these coatings was found to be related to the extent of Mo as well as the local anodes and cathodes. The amount of molybdenum in the Zn-Co-Mo coating varied from 2.6 to 14 wt.% as a result of changing the pH. Based on the experimental findings, a narrow range of pH values between 5 and 5.5 could contribute to the high quality of coating in conjunction with the corrosion resistant alloy. Besides, the coatings with Mo element could show a passive-like behavior in the anodic region.

Keywords corrosion, electrodeposition, galvanostatic deposition, Zn-Co-Mo alloy

1. Introduction

In recent years, electrodeposition of alloys has been widely used in many industries with distinct advantages compared to other coating technologies such as sputtering and vapor deposition (Ref 1, 2). Zinc and its alloy deposits are commonly used to protect the steels against the corrosion (Ref 3). These coatings have attracted scholars' attention as the replacement materials for the cadmium coatings or Cr(VI)-based conversion layers (Ref 4).

Electrodeposition of binary Zn-M alloys, where M is an iron group metal (Fe, Co or Ni), has been extensively studied with the results demonstrating the enhanced properties compared to the pure Zn (Ref 5). Because of the relatively large difference in the electronegativity of Zn and the steels, rapid dissolution of Zn occurs in the short lifetime of the coating under the corroding conditions. Alloying with an iron group metal would bring E_0 of the coating closer to the substrate and would

therefore lead to an increase in the durability of the coating (Ref 6).

Molybdenum has a beneficial effect on the properties of metallic coatings, improving their hardness and corrosion resistance. It is anticipated that molybdenum will also favorably influence the properties of zinc coatings, especially their corrosion resistance. Nevertheless, molybdenum cannot be electrodeposited in the pure state from the aqueous solution. It can be co-deposited with some metals, especially the iron group metals (Ref 7, 8). Molybdenum can be introduced into the zinc coatings by co-depositing it with iron group metals (Fe, Co, Ni). The ternary Zn-Co-Mo alloy coatings were deposited from a weak acid sulfate or citrate-sulfate baths, which led to the formation of bright homogeneous coatings in a narrow range of pH (Ref 9). It has been demonstrated that the ternary Zn-Co-Mo alloy coatings which contained small percentages of Mo and Co exhibited much better mechanical and corrosion properties in the chloride media than the zinc coatings (Ref 7, 9).

A few studies have been conducted on the electrodeposition of Zn-Co-Mo coatings and their properties (Ref 7, 9). Zn-Co-Mo alloy coatings were deposited from a citrate-sulfate bath in a pH range of 5.5-5.9. The obtained coatings possessed 2.3-3.6 wt.% Mo and 3.4-3.7 wt.% Co. However, the extent of Mo content as the corrosion resistant alloy was low (about 5 wt.%) (Ref 7). Therefore, this study mainly aims at investigating the deposition of ternary alloy with the Mo content higher than 5 wt.% in a simple citrate bath in order to obtain a corrosion resistant Zn-Co-Mo coating. In this work, the effect of pH on the composition, morphology, and corrosion resistance of galvanostatic electrodeposited Zn-Co-Mo coatings was studied. For this purpose, SEM, EDX, XRD, DC polarization, CV, and EIS measurements of the Zn-Co-Mo alloy coatings were taken. The corrosion resistance of the modified ternary coatings was compared to the steel substrate in the NaCl solution.

A. Keyvani, Department of Metallurgy and Materials Engineering, Faculty of Technology and Engineering, Shahrekord University, P.O. Box 115, Shahrekord, Iran; M. Yeganeh, Department of Materials Science and Engineering, Faculty of Engineering, Shahid Chamran University of Ahvaz, Ahvaz, Iran; and H. Rezaeyan, Corrosion Laboratory, School of Metallurgy and Materials Engineering, University College of Engineering, University of Tehran, Tehran, Iran. Contact e-mails: Keyvani@eng.sku.ac.ir and akeyvani@ut.ac.ir.

2. Experimental

Zn-Co-Mo alloy coatings were deposited from a citrate bath. All the reagents were of analytical grade and were used without further purification. The pH of the electrolytes was adjusted to 3.5, 4, 4.5, 5, and 5.5 using a solution of H_2SO_4 or NH_4OH . The concentrations of ZnSO_4 , CoSO_4 , Na_2MoO_4 , and $\text{Na}_3\text{C}_6\text{H}_5\text{O}_7$ were chosen 0.1, 0.1, 0.01, and 0.2 M, respectively. The coatings were deposited on the 3-cm² electrodes made of carbon steel plate. The steel plates (composition in wt.%: Fe: 97.7, C: 0.19, Si: 0.415, Mn: 1.39, $P < 0.005$, $S < 0.005$, Cr: 0.026, Mo: 0.018, Co: 0.0559, Cu: 0.0429, Nb: 0.0481) were polished with SiC papers (# 100 up to 1200) and carefully degreased with acetone, followed by water rinsing and drying. The steel electrodes were chemically polished using a solution of oxalic acid and 30% solution of hydrogen peroxide (the mixture of 14 cm³ oxalic acid 100 g dm⁻³ with 2 cm³ 30% H_2O_2 and 40 cm³ H_2O). The electrodeposition tests were performed in a three-electrode cell using potentiostat EG&G 273A. The coatings were deposited in a 100-cm³ beaker at a temperature of 25 °C under galvanostatic conditions at a current density of 10 mA cm⁻². The quality of coating in the lower current density was not appropriate. On the other hand, hydrogen evolution led to the coating deterioration at higher current densities. Cyclic voltammetry technique was used in the potential range of 0 to -2000 mV. The scan rate was chosen 20 mV s⁻¹.

The surface morphology of the coatings was analyzed by SEM (Zeiss). The chemical composition of the samples was measured using Oxford energy-dispersive spectroscopy. The crystalline structure of the coated samples was analyzed using a Philips X'Pert-Pro instrument operating at 40 kV and 30 mA with $\text{CuK}\alpha$ radiation in the angle range of 20°-120° and 0.02° as the step size. The electrochemical measurements were taken in a classical electrochemical cell with the steel plates coated by alloy films as the working electrode with an exposed area of 1 cm². While an Ag/AgCl electrode was taken as a reference electrode, a platinum plate was used as the counter electrode. Electrochemical impedance spectroscopy (EIS) tests were conducted at the open circuit potential (OCP) by immersing specimens into the 0.1-M NaCl. The AC amplitude was 5 mV, and the frequency was set in the range of 100 kHz to 10 mHz using a 1260 Solartron frequency response analyzer (FRA). ZView 3.1c software was used to analyze EIS data. All OCP tests were performed on an EG&G potentiostat-galvanostat 273A model equipment controlled by software M352. Potentiodynamic polarization curves were obtained by the scanning of potential from -500 to 1000 mV versus Ag/AgCl with a scan rate of 1 mV s⁻¹. Corrosion current density (I_{corr}) was determined using the software M352. All electrochemical tests were done at least three times to ensure data output accuracy.

3. Results and Discussion

Figure 1(a), (b), (c), (d), and (e) shows the SEM morphology of Zn-Co-Mo coatings after deposition in the citrate solution with the pH values adjusted at 3.5, 4, 4.5, 5, and 5.5 at the current density of 10 mA cm⁻². As shown in this figure, at the lowest pH, the deposit showed a hexagonal plate-like morphology, which could be due to the presence of a high

amount of zinc. Zinc morphology disappeared by increasing the pH value higher than 4 (Fig. 1c, d, e), and an ultra-fined structure substituted. Figure 2(a), (b), (c), (d), and (e) presents the EDS spectra regarding the Zn-Co-Mo coatings. The compositions of Zn-Co-Mo coatings in different pHs are listed in Table 1.

As shown in Table 1, the amount of Mo in the coating varied as a result of changing the pH content. As shown in this table, Mo was not deposited in the coating at low pHs such as 3.5 and 4. At more acidic pH, the amount of deposited Zn was higher than the other elements, which emphasized an anomalous deposition (Ref 10). However, Higashi et al. (Ref 11) proposed that the formation of zinc hydroxide on the cathode surface could restrict the discharge of other metals on the cathode surface, leading to the anomalous deposition. This zinc hydroxide film was formed due to an increase in the interfacial pH during the simultaneous electrochemical reaction of hydrogen evolution. This effect can also be explained by the fact that the exchange current densities of the iron group metals (Fe, Co, Ni) were lower than that of zinc, which favored the preferential deposition of zinc (Ref 12).

The content of Mo in the pH range of 5-5.5 had a high value in the coating composition, which could be associated with the creation of various complex compounds in the electroplating bath. The stable homogenous solution was obtained in a narrow pH range with the electroactive complexes. The citrate baths with the pHs higher than 6 possessed mainly non-electroactive complexes of zinc, which resulted in the lowest deposition of zinc. Besides, zinc hydroxide was formed at higher pH values in the solution (Ref 13). This behavior led to having to choose a narrow pH range (5-5.5 in this study) for electrodeposition of Zn-Co-Mo alloy. On the other hand, the baths with the pHs below 4 were not stable because sparingly soluble polymeric citrate complexes of zinc and polymeric molybdenum (VI) compounds were formed (Ref 13). However, as shown in Table 1, deposition in the lower pH was anomalous, which led to the higher zinc deposition. Each variation in the parameters including pH and electrolyte concentration could change the complex charge, and therefore, the content of alloying elements in the coating varied. For example, increasing the pH from 5 to 6 could change $[\text{ZnHcit}]^-$ to $[\text{Zn}_2\text{cit}]^0$ in the 0.1-M citrate sodium which resulted from variations in the presence of zinc element in the coatings (Ref 13).

Figure 3 shows cathodic polarization of Zn, Co, Mo, and Zn-Co-Mo in the citrate bath at the pH of 5.5. As can be observed in this figure, at every negative potential from the OCP, the current density of the elements was different due to the anomalous behavior of Zn-Co-Mo coating. However, at some points, the related current densities of Co and Mo were equal, which could be attributed to the induced deposition of Mo with the iron group. This figure also demonstrates that, around -1.1 V versus Ag/AgCl, the current density regarding Co and Mo is identical. Therefore, it could be expected that the deposition of this alloy by applying any negative potential was not feasible.

Figure 4 shows the cyclic voltammetry (CV) plot for the deposition of Zn-Co-Mo at the pH of 5.5. The potential of this CV plot varies from 0 to -2 V versus Ag/AgCl and shows some different peaks in the cathodic region. As this alloy could not form a solid solution in the deposition stage due to the formation of complex compounds between these elements, the cyclic voltammetry could exhibit some different peaks related to the reduction in different compounds on the surface. These

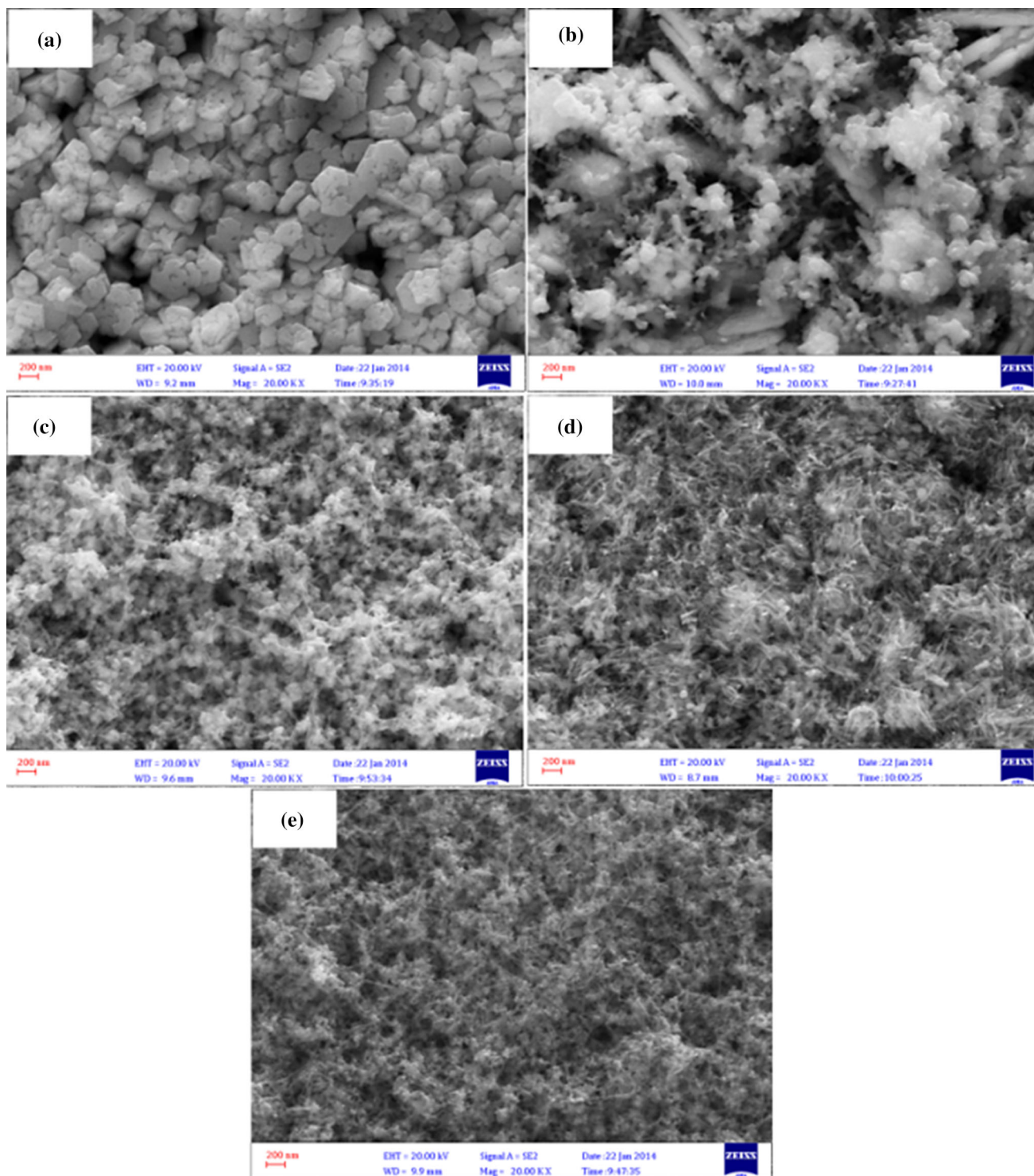


Fig. 1 Surface morphology of Zn-Co-Mo coatings deposited at 10 mA cm^{-2} with different pHs: (a) 3.5, (b) 4, (c) 4.5, (d) 5, and (e) 5.5

Table 1 Variations of the Zn-Co-Mo composition by pH and the current density of 10 mA cm^{-2}

pH	Zn, wt.%	Co, wt.%	Mo, wt.%	Thickness, μm
3.5	97.7	2.3
4	96.6	3.4
4.5	94.6	2.8	2.6	4.1
5	64	22	14	3.5
5.5	87.4	5.6	7	3.9

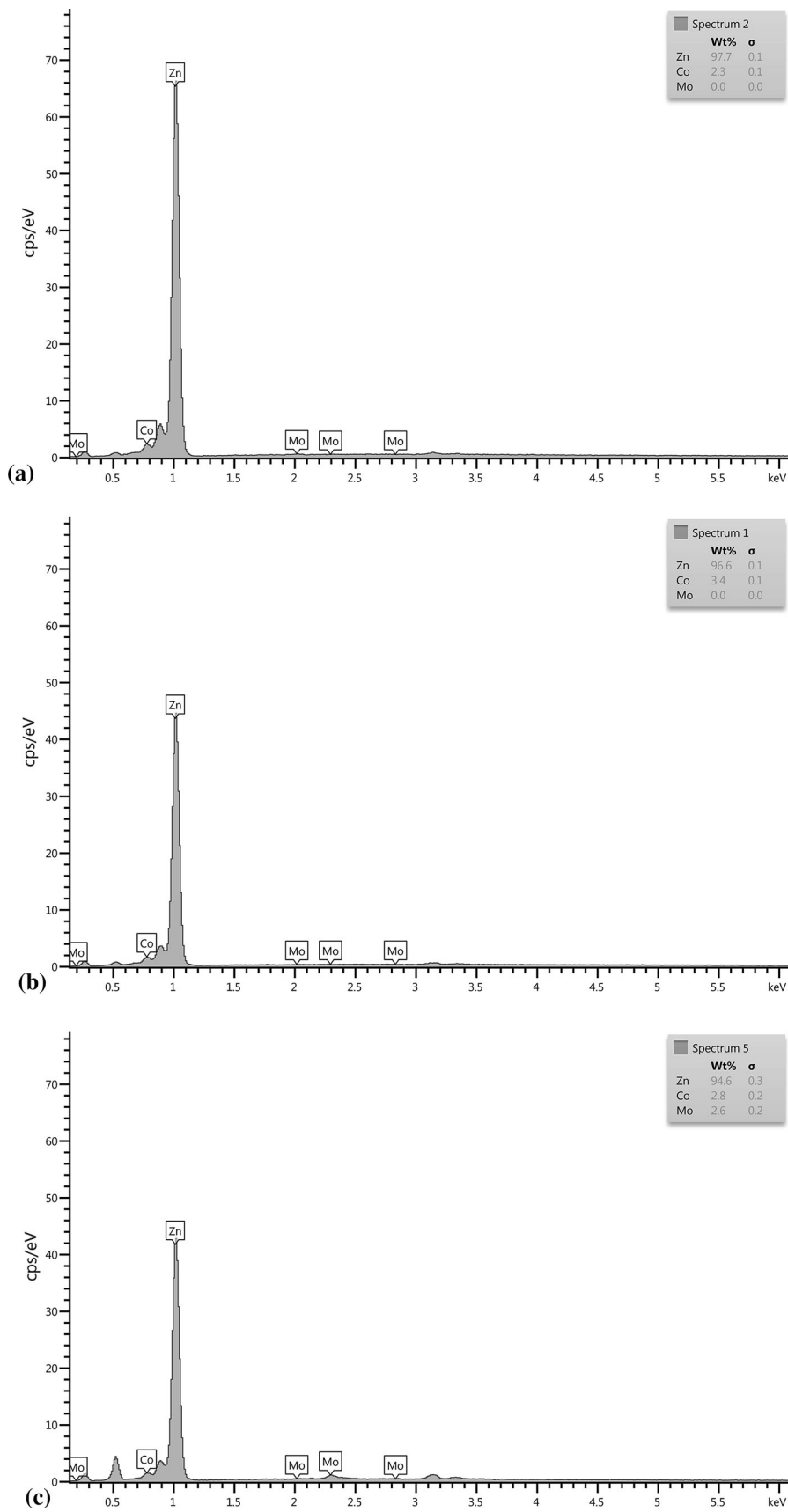


Fig. 2 EDS spectra related to Zn-Co-Mo coatings deposited at 10 mA cm^{-2} with different pHs: (a) 3.5, (b) 4, (c) 4.5, (d) 5, and (e) 5.5

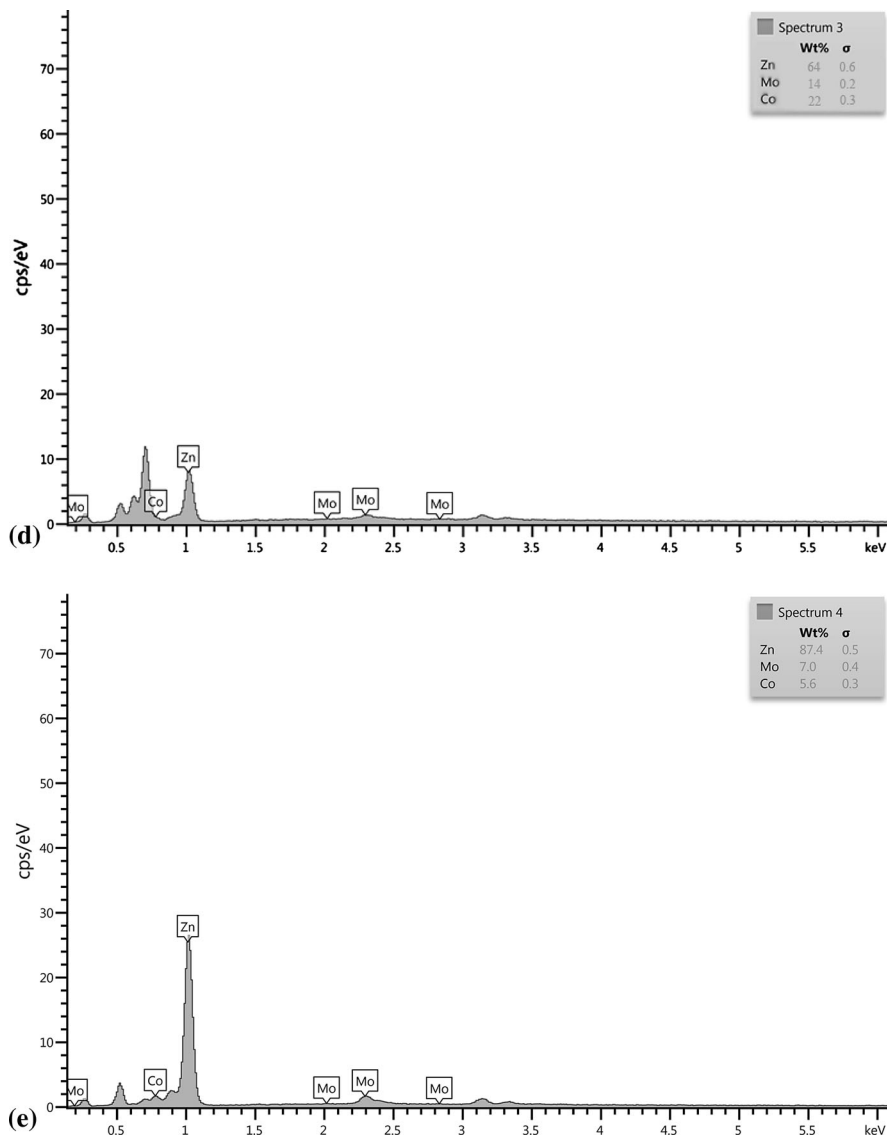


Fig. 2 continued

peaks could be related to the various stages of complex reduction such as $[\text{ZnHcit}]^-$, $[\text{Zn}_2\text{cit}]^0$ or complicated Mo complexes (Ref 13, 14).

Figure 5 presents the galvanostatic curves for the deposition of Zn-Co-Mo alloys with the different pH of bath using the current density of 10 mA cm^{-2} . It can be seen that the deposition potential greatly depended on the pH of the plating bath, which was a sign of charges in the electrolyte. As can be observed, the Zn-Co-Mo alloy deposited mainly in negative potentials higher than -1.27 V versus Ag/AgCl. It seemed that at lower pHs, the required time for the beginning of stable deposition was higher, which could be explained by the presence of sparingly soluble polymeric citrate complexes of zinc and polymeric molybdenum (VI) compounds (Ref 13). However, the observed potential fluctuations in the galvanostatic curves were probably due to the hydrogen evolution.

The thickness of electroplated coatings could be calculated from Eq 1:

$$h = \frac{m_t}{d_a A} \quad (\text{Eq 1})$$

where h is the evaluated thickness, m_t is the total mass of deposit, A is the deposited surface, and d_a is the alloy density. However, m_t could be estimated from Faraday law ($m_t = ItM/nF$). In this law, I is the current passing through the electrode, t is the time, M is the molar mass, n is the valence of the element, and F is the Faraday constant. Thus, the thickness of Zn-Co-Mo coating at the pH of 4.5, 5, and 5.5 could be estimated by Eq 2:

$$h = \frac{It(\text{wt.}\% \text{Zn} \cdot M_{\text{Zn}}/2 + \text{wt.}\% \text{Co} \cdot M_{\text{Co}}/2 + \text{wt.}\% \text{Mo} \cdot M_{\text{Mo}}/6)}{F \cdot A \cdot (\text{wt.}\% \text{Zn} \cdot d_{\text{Zn}} + \text{wt.}\% \text{Co} \cdot d_{\text{Co}} + \text{wt.}\% \text{Mo} \cdot d_{\text{Mo}})} \quad (\text{Eq 2})$$

The thickness of the coatings deposited at pHs of 4.5, 5, and 5.5 was calculated to be 4.1, 3.5, and 3.9 μm , respectively. These Zn-Co-Mo coatings showed a close thickness to each other.

Table 2 Impedance data obtained from ZView simulation for the steel and the coatings in the chloride media

Specimen	pH	Rect, $\Omega \text{ cm}^2$	CPE _{ct} , $S - s''$	$W_s - R, \Omega \text{ cm}^2$	$W_s - T, s$	$W_s - P$	χ^2
Steel	...	1370	1.6E-5	0.001
Coatings	4.5	4220	3.2E-6	1241	124	0.43	0.004
	5	5810	2.1E-6	1941	320	0.63	0.01
	5.5	6750	1E-6	3011	123	0.78	0.005

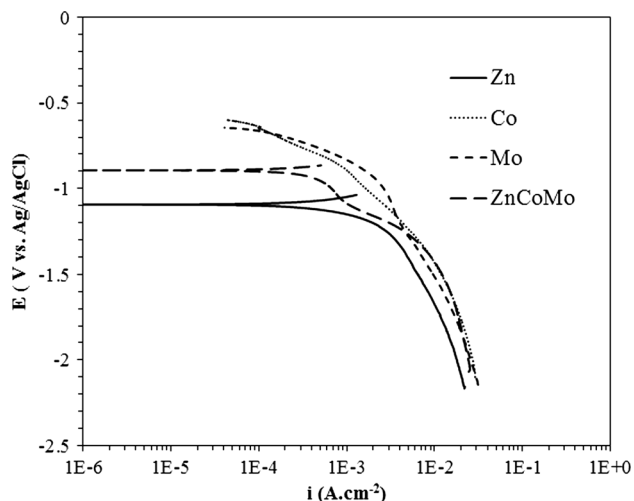


Fig. 3 Cathodic polarization plots for Zn, Co, Mo, and Zn-Co-Mo alloy in citrate bath at pH 5.5

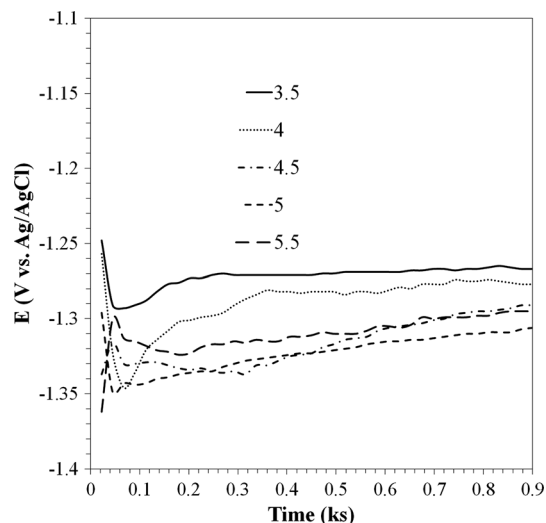


Fig. 5 Galvanostatic curves for Zn-Co-Mo electrodeposition in different pHs

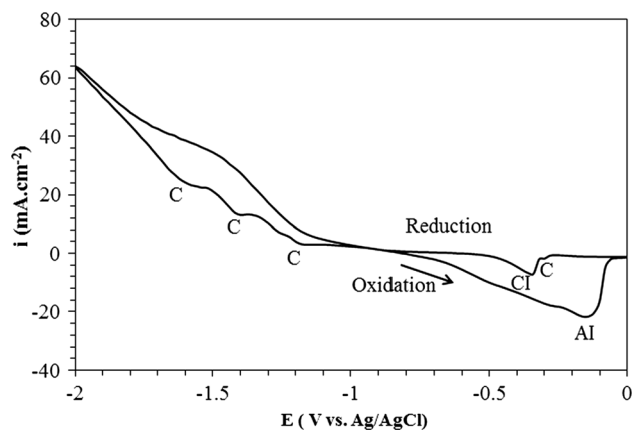


Fig. 4 Cyclic voltammetry diagram for Zn-Co-Mo deposition at pH of 5.5

The XRD patterns of the steel substrate and the Zn-Co-Mo coating deposited at pH 5.5 are shown in Fig. 6(a) and (b), respectively. As can be observed in these figures, the deposited coatings exhibit a crystalline structure. The peaks at 2θ of 43.1° and 82.7° belonged to Zn-Co-Mo coating and the peaks at 2θ of 44.8° , 65.5° , and 82.9° were characteristic of Fe (JCPD no: 06-0696). However, a few peaks for Zn planes were slightly shifted to lower angle degrees (Fig. 6b), which could suggest the appearance of a zinc-rich phase. Cobalt and molybdenum atoms could have been substituted into the zinc lattice, which led to a distortion of the zinc crystal structure. The peaks at about $2\theta = 36.9^\circ$ and 41.1° regarding Zn-Co-Mo coating

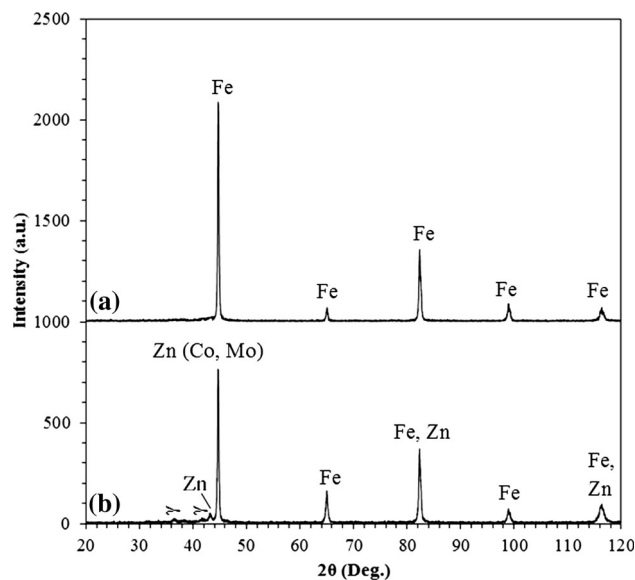


Fig. 6 XRD diffractograms of (a) the steel substrate and (b) Zn-Co-Mo alloy (5.6 wt.% Co, 7 wt.% Mo) coating deposited at pH 5.5

(Fig. 4b) might be due to the formation of CoZn_{13} phase (γ) (JCPD No: 65-1237) (Ref 7).

Figure 7 shows the Nyquist plot for the steel and Zn-Co-Mo deposited at the pHs of 4.5, 5, and 5.5 in the 0.1-M NaCl. As shown in Fig. 8(a) and (b), two types of equivalent circuits were proposed for the corrosion of the steel and the coatings in the chloride solutions, respectively.

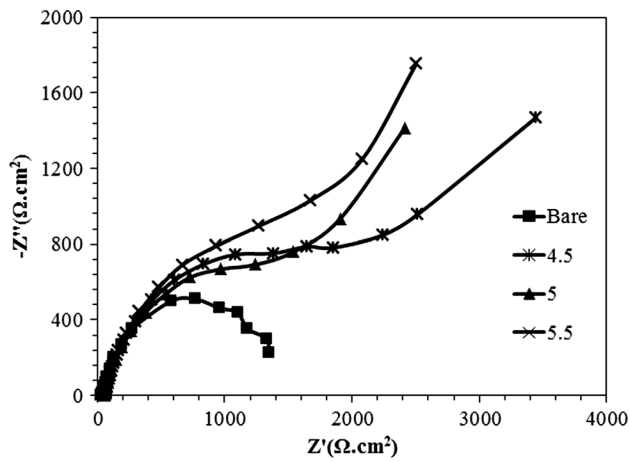


Fig. 7 Nyquist curves for the coatings deposited at pHs 4.5, 5, and 5.5 in comparison with bare steel after immersion in 0.1 M NaCl

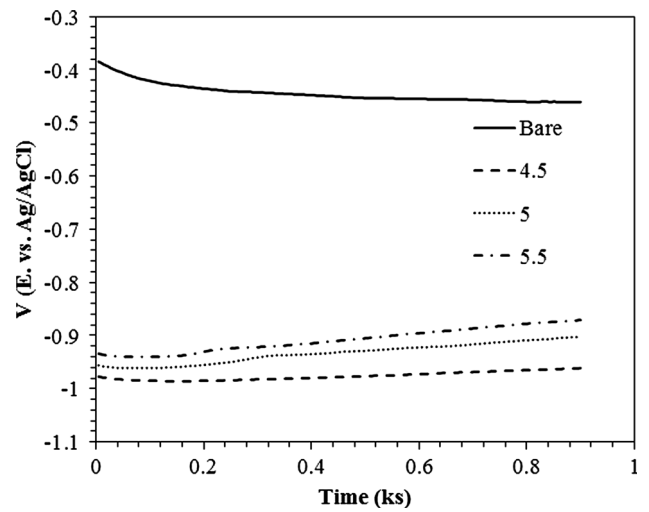


Fig. 9 OCP plots for Zn-Co-Mo coatings after immersion in chloride media

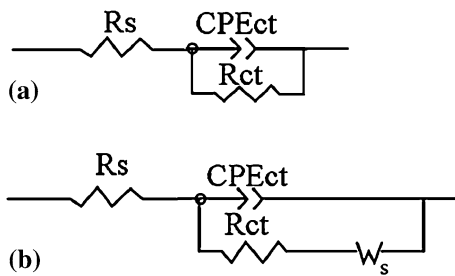


Fig. 8 Equivalent circuits for (a) bare steel and (b) Zn-Co-Mo coating after immersion in NaCl solution

Table 3 I_{corr} and E_{corr} for the coatings and bare steel after the immersion in the NaCl solution

Sample	pH	I_{corr} $\mu A\ cm^{-2}$	E_{corr} mV vs. Ag/AgCl
Steel	...	70.1	-323
Coatings	4.5	9.3	-1006
	5	4	-941
	5.5	3.9	-940

In these circuits, R_s is the solution resistance. R_{ct} represents the charge transfer resistance, which is parallel with a constant phase element (CPE). CPE is applied instead of a pure capacitance due to the non-ideal capacitive response of the interface in the solution. The impedance of a CPE is equal to $[Q(j\omega)^n]^{-1}$, where Q is the constant corresponding to the interfacial capacitance, j is the imaginary number, ω is the angular frequency, and n is an exponential factor in the range between 0 and 1 (Ref 15). CPE is in parallel with R_{ct} and W (W represents the Warburg impedance). This impedance implies the ion transport across the system or diffusion of the electroactive species through the pores of the coating (Ref 15). Warburg impedance emphasizes the corrosion under diffusion control. Uniform coated steel was characterized by the higher R_{ct} and Warburg impedance W . As seen in these curves, the steel showed a loop regarding its charge transfer resistance while the coatings showed a loop at higher

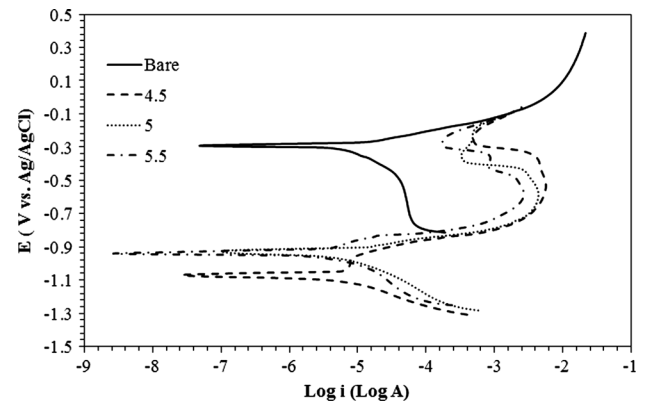


Fig. 10 Polarization curves for the coatings deposited at pH 4.5, 5, and 5.5 in comparison with bare steel after immersion in 0.1 M NaCl

Table 4 Content of elements in the Zn-Co-Mo composition after corrosion in the NaCl solution

Sample	pH	Zn	Co	Mo
Zn-Co-Mo	4.5	73	14	13
	5	62	22	16
	5.5	85	5	10

frequencies and a tail according to Warburg diffusion at lower frequencies. This impedance exhibited a barrier mechanism slower than the charge transfer for the coatings (Ref 15). The optimized values regarding the parameters of equivalent circuits, which were obtained from ZView software, are summarized in Table 2. These parameters were fitted well indicated by a low Chi-squared (χ^2) value which is the value of the curve fitting parameter. The contents of χ^2 were obtained in the range of 0.001-0.01. Charge transfer resistance for the steel was obtained to be 1370 $\Omega\ cm$. However, the corresponding values for Zn-Co-Mo coatings deposited at the pHs of 4.5, 5, and 5.5 were 4220, 5810, and 6750 $\Omega\ cm^2$, respectively. It

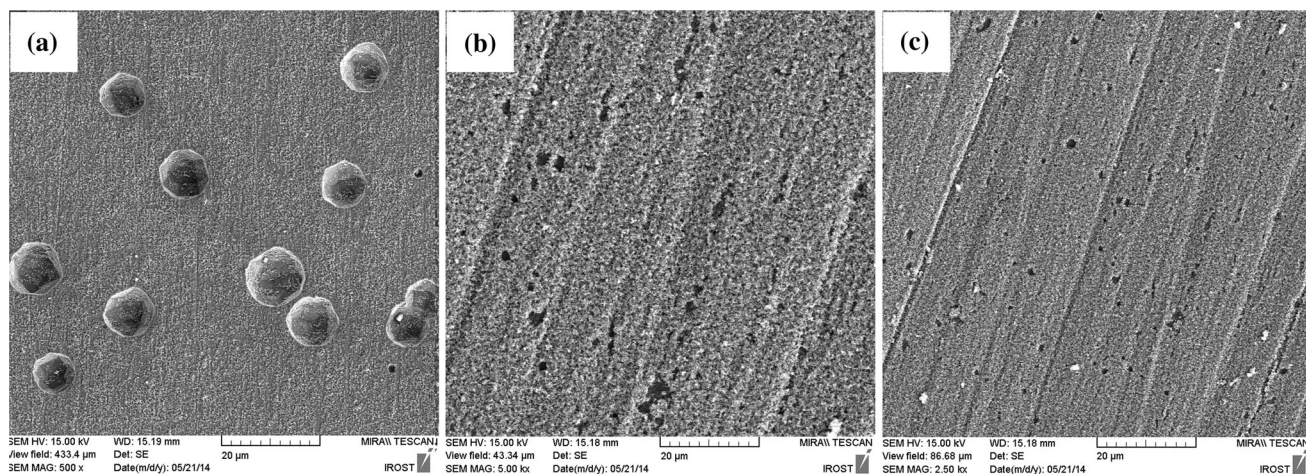


Fig. 11 Surface morphology of Zn-Co-Mo coatings deposited at different bath pH: (a) 4.5, (b) 5, and (c) 5.5 after corrosion in NaCl solution

could be concluded that these coatings had a better corrosion resistance in comparison with the bare steel, which might be attributed to the presence of Mo in the composition of the coatings.

Figure 9 shows the OCP of Zn-Co-Mo coatings deposited at the pHs of 4.5, 5, and 5.5 compared to the bare steel in the 0.1-M NaCl solution. The lower OCP of the coatings could be attributed to the presence of Zn with a higher negative standard potential. As shown in this figure, the coating which was fabricated at the pH of 4.5 possessed the lowest OCP. This could be due to the highest value of Zn and the lowest value of Mo. Therefore, it can be concluded that the OCP data give some information about the presence of active or noble elements in these Zn-Co-Mo coatings. Alloying Zn with cobalt (Co) and molybdenum (Mo) made the total E_0 closer to the steel substrate with the reduction in the driving force for dissolution and therefore enhanced the corrosion resistance of Zn-Co-Mo coatings.

Figure 10 shows the polarization diagrams for the coatings and the bare steel in the 0.1-M NaCl solution. As shown in this figure, the coatings showed a more negative OCP than the bare steel. Besides, they showed a passive-like behavior in the anodic region, which could be due to the formation of Mo compositions in these zones. As can be observed in Fig. 10, all of the samples with the Mo content illustrated a passive-like behavior. Comparing these findings with the results presented by Kanda et al. (Ref 16) and Szczygieł et al. (Ref 8) shows that the improved corrosion resistance of alloy coatings resulted from the presence of a passive layer which consisted of a molybdenum-rich compound.

All coatings showed the lower corrosion current density in comparison with the bare steel substrate, which was a sign of the formation of a good protective compound on the surface of the steel. The coating deposited at the pH of 4.5 showed the highest corrosion current density in comparison with the other coatings, emphasizing the lower Mo content. Table 3 shows I_{corr} and E_{corr} for the bare steel and the coatings in the NaCl solution. As shown in this table, the coating deposited at the pHs of 5 and 5.5 possessed the lowest I_{corr} . The Zn-Co-Mo coating deposited at the pH of 5 showed the highest current density in the widest range of anodic potentials compared to the

coating deposited at the pH of 5.5. The amount of recorded current for Zn-Co-Mo coating deposited at the pH of 5.5 was lower in the most anodic potentials in comparison with the other coatings. Seemingly, a little amount of Mo can contribute to the formation of the passive layer. However, when the amount of Mo exceeded the critical value, it resulted in the formation of local anodic and cathodic zones, which could accelerate the corrosion rate in the higher anodic potentials. Therefore, it was found that the coating deposited at the pH of 5.5 exhibited the best corrosion resistance as well as the optimum Mo content.

Figure 11(a), (b), and (c) shows the surface morphology of Zn-Co-Mo coatings after immersion in the NaCl solution. Table 4 summarizes the content of Zn-Co-Mo coatings after corrosion in the NaCl solution. The coating at the pH of 4.5 (Fig. 11a) showed a lower corrosion resistance compared to other samples due to the lower Mo content. The amount of Mo after the corrosion increased due to the dissolution of Zn or Co elements. The observed pits on the surface of this coating are a good reason for this claim. The other coatings (Fig. 11b, c) exhibited the smaller pits, and their composition did not change drastically after corrosion. As mentioned earlier, this could be explained by the formation of a protective layer during the corrosion damages.

4. Conclusion

In this study, Zn-Co-Mo alloy was deposited from citrate bath solution with different pHs. The results showed that the amount of Mo depended on the pH of the considered bath. Consequently, it was found that the best pH range for alloy deposition was in the range of 5-5.5. According to the results of the experiments, Zn-Co-Mo alloy was more likely to deposit at least in the potential of -1.25 V versus Ag/AgCl. It is worth mentioning here that the corrosion resistance of deposits was associated with their Mo content. Nonetheless, the highest amount of Mo could not contribute to the maximum level of resistivity due to the generation of several local anodic and cathodic sites as a consequence of the high amount of Mo in the deposit. More precisely, the corrosion resistance of the alloy

containing Mo was ascribed to the formation of the passive layer with a Mo-rich composition.

References

1. J.B. Bajat, S. Stanković, and B.M. Jokić, Electrochemical Deposition and Corrosion Stability of Zn-Co Alloys, *J. Solid State Electrochem.*, 2009, **13**, p 755–762
2. R. Lopez Anton, M.L. Fdez Gubieda, A. Garcia-Arribas, J. Herreros, and M. Insausti, Preparation and Characterisation of Cu-Co Heterogeneous Alloys by Potentiostatic Electrodeposition, *Mater. Sci. Eng. A*, 2002, **335**, p 94–100
3. J.L.O. Aparicio, Y. Measa, G. Trejoa, R. Ortega, T.W. Chapman, E. Chainet, and P. Ozilb, ZnCo-Electrodeposition Baths Based on Alkaline Chloride-Gluconate Electrolytes Containing Quaternary Ammonium Compounds, *J. Electrochem. Soc.*, 2009, **156**, p 205–213
4. H. Kazimierzczak and P. Ozga, Electrodeposition of Sn-Zn and Sn-Zn-Mo Layers from Citrate Solutions, *Surf. Sci.*, 2013, **607**, p 33–38
5. N. Boshkov, N. Boshkova, V. Bachvarov, M. Peshova, and L. Lutov, Corrosion Investigations of Black Chromite Films on Zn and Zn-Co Coatings with Low Cobalt Content, *J. Mater. Eng. Perform.*, 2015, **24**, p 4736–4745
6. Z.F. Lodhi, J.M.C. Mol, A. Hovestad, L. Hoen-Velterop, H. Terryn, and J.H.W. de Wit, Corrosion Resistance of Zn-Co-Fe Alloy Coatings on High Strength Steel, *Surf. Coat. Technol.*, 2009, **203**, p 1415–1422
7. J. Winiarski, W. Tylus, K. Winiarska, and B. Szczygieł, The Influence of Molybdenum on the Corrosion Resistance of Ternary Zn-Co-Mo Alloy Coatings Deposited from Citrate-Sulphate Bath, *Corros. Sci.*, 2015, **91**, p 330–340
8. B. Szczygieł, A. Laszczyński, and W. Tylus, Influence of Molybdenum on Properties of Zn-Ni and Zn-Co Alloy Coatings, *Surf. Coat. Technol.*, 2010, **204**, p 1438–1444
9. J. Winiarski, W. Tylus, and B. Szczygieł, EIS and XPS Investigations on the Corrosion Mechanism of Ternary Zn-Co-Mo Alloy Coatings in NaCl Solution, *Appl. Surf. Sci.*, 2016, **364**, p 455–466
10. A. Brenner, *Electrodeposition of Alloys, Vols. 1 and 2*, Academic Press, New York, 1963
11. K. Higashi, H. Fukushima, T. Urakawa, T. Adaniya, and K. Matsudo, Mechanism of the Electrodeposition of Zinc Alloys Containing a Small Amount of Cobalt, *J. Electrochem. Soc.*, 1981, **128**, p 2081–2085
12. R. Fratesi and G. Roventi, Electrodeposition of Zinc-Nickel Alloy Coatings from a Chloride Bath Containing NH₄Cl, *J. Appl. Electrochem.*, 1992, **22**, p 657–662
13. H. Kazimierzczak, P. Ozga, and R.P. Socha, Investigation of Electrochemical Co-deposition of Zinc and Molybdenum from Citrate Solutions, *Electrochim. Acta*, 2013, **104**, p 378–390
14. P. Amico, P.G. Daniele, G. Ostacoli, G. Arena, E. Rizzarelli, and S. Sammartano, Mixed Metal Complexes in Solution. Part 4. Formation and Stability of Heterobinuclear Complexes of Cadmium(II)-Citrate with Some Bivalent Metal Ions in Aqueous Solution, *Trans. Met. Chem.*, 1985, **10**, p 11–14
15. M. Saremi and M. Yeganeh, Application of Mesoporous Silica Nanocontainers as Smart Host of Corrosion Inhibitor in Polypyrrole Coatings, *Corros. Sci.*, 2014, **86**, p 159–170
16. K. Kanda and K. Saijo, Chemical State Analysis of Zn-Co-Mo Electroplated Layers by x-ray Photoelectron Spectroscopy, *J. Met. Finish. Soc. Jpn.*, 1984, **35**, p 230–235